Assessment of Impact Damage Resistance and Tolerance of Polymer Nanofiber Interleaved Composite Laminates

Paul Akangah[1], Kunigal Shivakumar

NASA Center for Aviation Safety, North Carolina A & T State University,1601 East Market Street, 205 Fort IRC Bldg, Greensboro, NC 27411, USA

[1]pmakanga@ncat.edu

***Abstract*-Polymer nanofiber interleaving is a novel technology to enhance toughness of composite laminates. This paper focuses on the comparison of low velocity impact damage resistance and tolerance of base (no interleaving) and polymer nanofiber interleaved composite laminates. A 24-ply aerospace grade AS4/3501-6 Carbon/Epoxy laminate was made in an autoclave. The interleaved laminate was made by placing a layer of Nylon-66 nanofiber between the adjacent plies and at the top and bottom of the laminate. The nanofabric was made by electrospinning 12% wt. of Nylon-66 solution made by dissolving Nylon-66 crystals in a mixture of 90% formic acid and chloroform in a weight ratio of 75/25, respectively. The average areal density of the fabric was 0.7 g/m^2 and the AS4/3501-6 composite ply was 260 g/m^2. Impacted panels were c-scanned and the measured damage of the two laminates was compared with each other. Compression was implemented to the specimens for impact test to measure the damage tolerance. Results showed that polymer nanofiber interleaving does have a potential to improve impact damage resistance and tolerance. Specifically, interleaving increased the threshold impact force by about 12% and the compression strength by about 10%.**

Keywords- Nanofiber; Impact Damage; Impact Resistance; Interleaving

NOMENCLATURE

CAI	=	compression after impact
D	=	distance between the tip of the syringe needle and the collector, mm
D_a	=	damage area, mm^2
E, E_0, E_a, E_c	=	impact, maximum, dissipated and critical energy, J
F_{1C}	=	weighted compressive strength of pristine laminate, MPa
F_{CAI}	=	ultimate compressive residual strength, MPa
g	=	acceleration due to gravity, 9.81 m/s^2
h	=	specimen thickness, mm
H	=	impact height, mm
HV	=	high voltage DC source
k_b, k_m, k_s, k_c	=	bending, membrane, shear and contact stiffness, N/m
k_{bs}	=	bending and shear effective stiffness, N/m
M	=	impactor mass, kg
M_p	=	specimen test section mass, kg
P_0	=	maximum force (analysis), N
P_c, P_{max}	=	critical and maximum force, N
P_{cmax}	=	maximum compressive force, N
R	=	radius of rotating drum, mm
SDOF	=	single degree of freedom
SEM	=	scanning electron microscope
t	=	time, s
V	=	applied voltage, kV

V_0 = impact velocity, m/s

W = specimen out-of-plane displacement, mm

w = specimen width, mm

I. INTRODUCTION

The primary limitation of fiber reinforced composite laminates is their poor interlaminar strength and fracture toughness, which results in poor impact damage resistance and tolerance[1,2]. A number of techniques have been attempted to improve the interlaminar strength and toughness, and to mitigate edge stresses. These methods include matrix-toughening[3], optimizing stacking sequence[4], stitching of laminates[5,6], using braided fabric[6], reinforcing with edge caps[7], terminating of critical plies in the laminate[8], and replacing of stiff plies with soft plies. However, these methods are limited by factors such as increase in cost, weight, or loss of in-plane properties. A promising technique is interleaving[9]. Thermoplastic particle interleaving has been applied to toughen carbon fiber reinforced laminates to mitigate impact damage[10], but this has resulted in significant loss of in-plane properties. Shivakumar et al[11],Akangah, Lingaiah and Shivakumar[12], and Shivakumar, Chen and Ali[13] explored the many positive attributes of Nylon-66 polymer nanofiber interleaving. These include increased fracture toughness and resistance, increased impact damaged resistance, no loss of in-plane stiffness and strength, and no multiple glass transition temperatures. The results presented in Ref.[12] were for exploratory study at low impact energy levels using an in-house built simple instrumented cantilever impactor for small-sized specimens. But ASTM Standard impact test was not performed because of limited material availability. The present study is more detailed and conforms to the ASTM Standard D7136. The study used Dynatub Drop-weight Impact Tester and 24 ply composite laminate with a thickness of 4.12 mm. Both the damage size and the corresponding impact force/energy relation of the base and the interleaved composite laminates are measured and compared. The impact tested specimens were compression tested to measure the impact damage tolerance.

The objective of this study was to assess the impact damage resistance and tolerance of a 24 ply quasi-isotropic AS4/3501-6 Carbon/Epoxy composite laminate with and without Nylon-66 nanofibers interleaving. An improved electrospinning set-up was developed with a collector current management technique[14-22].The equipment was used to prepare the Nylon-66nanofabric.

II. MATERIALS AND FABRICATION

A. Materials

AS4/3501-6 prepreg supplied by Hexcel Composites was chosen as the base material to evaluate the effect of Nylon-66nanofiber interleaving on impact damage properties. The material is brittle and used in many aerospace applications. The Nylon-66 supplied by Dupont Company (Zytel 101, MW= 20,000 g/mol) was selected to prepare the nonwoven nanofabric by electros pinning[11, 12]. Nylon-66 has extremely high elongation to fracture, excellent adhesion to epoxy matrix, and high melting/softening temperature of 250ºC which is higher than AS4/3501-6 cure temperature of 177ºC. Thus the Nylon-66 fibers should be unaffected during the curing of the composite laminate.

SEM micrograph of the polymer nanofabric spun at a flow-rate of 0.4 ml/hris shown in Fig. 1 (aandb) at magnifications of 15k and 60k, respectively. The fiber diameters ranged from 65 to 120 nm[23].

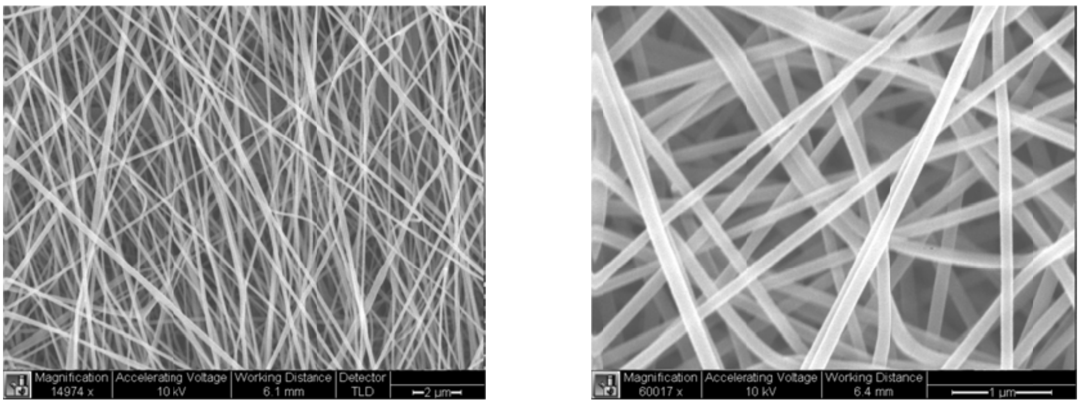

(a) 1.5k magnification (b) 60k magnification

Figure 1 SEM micrograph of fiber morphology

The range of electric field and minimum voltage required to produce minimum and consistent fiber diameters were found to be 1.6-1.7 kV/cm and 34.4-36.5 kV, respectively. The minimum distance between the tip of the needle and collector was established to be 21.5 cm[23].The electrospinning was done for 8 hours and the areal density of the fabric was 0.7 g/m^2. This represents 0.27% of the ply weight of AS4/3501-6 (42% resin weight) composite.

B. Fabrication of Panels and Test Specimens

A quasi-isotropic laminate of stacking sequence$^{[-45/90/45/0]}{}_{3S}$ was used for making the 24 ply laminates. Complete stacking sequence of the laminate and one set of each are shown in Figs. 2 and 3 for the base and interleaved laminates, respectively. The interleaved laminates were made by placing one layer of the nanofabric in between two consecutive prepreg layers. In addition, a layer of the nanofabric was also placed on the top and bottom surfaces of the laminate. These laminates were made in autoclave as per guidance provided by the prepreg supplier.

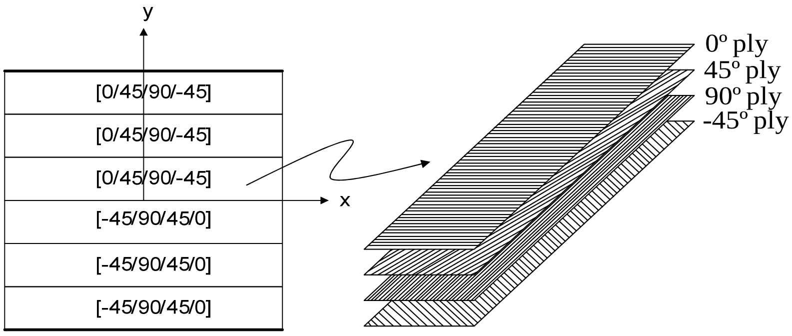

Figure 2 Schematic of base laminate stacking

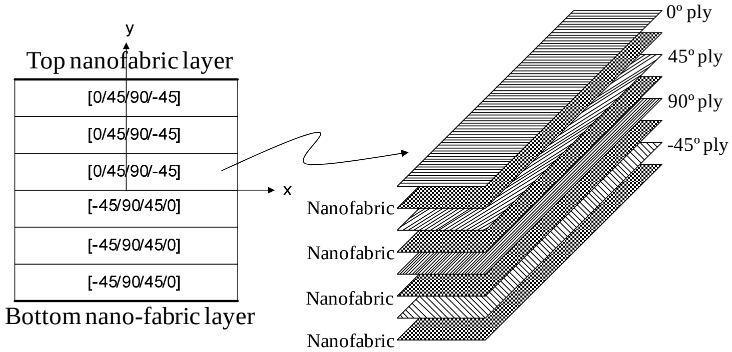

Figure 3 Schematic of interleaved laminate stacking

The average thickness of the laminate was 4.15 mm for the interleaved laminates and 4.14 mm for base AS4/3501-6 laminate. Averaged thickness difference between the base and interleaved AS4/3501-6 laminates was about 0.2%. Each laminate measured 356 mm x 762 mm (14 in x 30 in) and they were visually inspected for external damage and c-scanned for internal damage and were found to be satisfactory. The laminates were then cut into 70 test specimens (42 base and 28 interleaved test specimens) measuring 102 mm x 152 mm (4 in x 6 in).

III. IMPACT ANALYSIS OF LAMINATE

Mechanics of the drop weight tower setup is shown in Fig. 4. The impact process consists of two distinct states. In the first state, the impactor with effective mass, M, is raised to the impact height, H. At this state, the velocity of the impactor is zero and the potential energy is MgH, where g is the acceleration due to gravity (9.81 m/s^2).

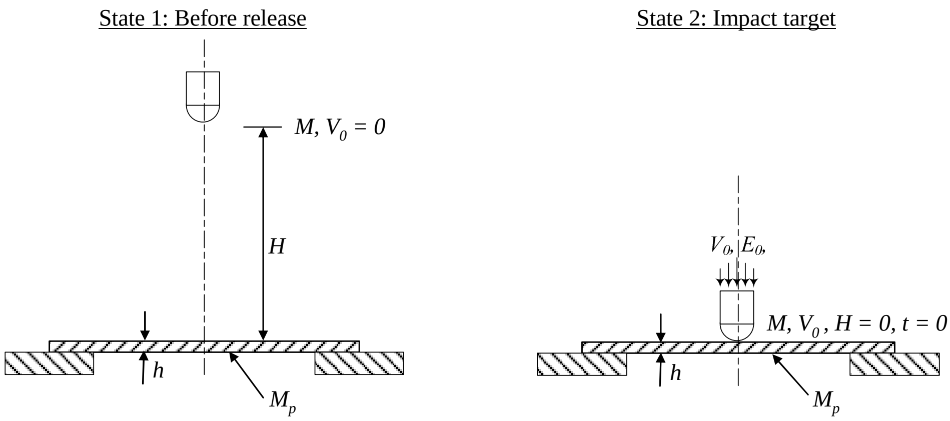

(a) Impactor positioned at impact height, H (b) Initial contact of impactor with laminate

Figure 4 Impact event in a drop weight tower setup

After releasing the impactor, it is accelerated by gravity and just before making impact with the test specimen (the time set to $t = 0$), the velocity $V(0) = V_0$ is measured by an infra-red detector and can also be calculated by equating the potential energy to the kinetic energy of the impactor. The second state is the contact deformation of the test specimen as the impact energy from the impactor is transferred to the specimen. The impactor is constrained to strike at the center of the rectangular test specimen, of mass M_p.

Figure 5 shows the schematic of the specimen deformation during impact. The deformation can be modeled by an equivalent nonlinear spring-mass model[24] shown in Fig. 6(a), where k_c, k_m, k_b and k_s are the contact, membrane, bending and shear stiffness, respectively. If geometric nonlinearities due to indentation, membrane, and damage are neglected, the nonlinear model will result ina single-degree-of-freedom (SDOF) model, shown in Fig. 6(b).

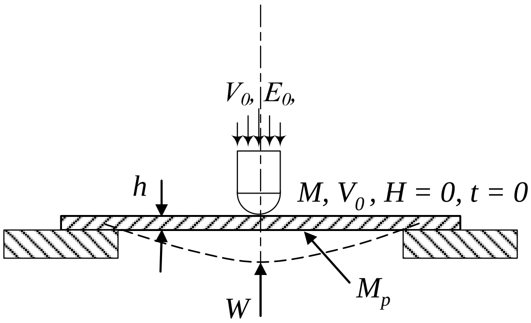

Figure 5 Schematic of specimen deformation during impact

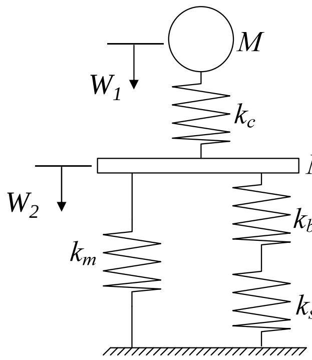

(a) Nonlinear contact model

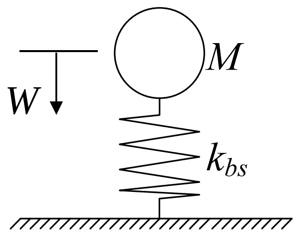

(b) Equivalent single-degree-of-freedom model

Figure 6 Spring-mass models

In the SDOF model, the impactor and laminate mass ratio must be greater than 2[26] and the combined bending-shear stiffness of the laminate is represented by the spring with equivalent stiffness (k_{bs}). The equation of motion for the SDOF model is given by:

$$M\ddot{W} + k_{bs}W = 0 \tag{1}$$

The assumed general solution to this free undamped system in Eq. (1) can be found in any text book on vibrations. Solving for the deflection (W), using the initial conditions; $V(0) = V_0$ and $W(0) = 0$, the exact solution is:

$$W(t) = \frac{V_0}{\omega}\sin\omega t \tag{2}$$

where $\omega = \sqrt{\frac{k_{bs}}{M}}$ is the fundamental frequency of the laminate in radians.The force-time response is given by:

$$P(t) = V_0 \left(k_{bs} M\right)^{0.5} \sin\left(\frac{\pi t}{T_0}\right) \tag{3}$$

where the contact duration, T_0, is defined as:

$$T_0 = \frac{\pi}{\omega} = \pi \sqrt{\frac{M}{k_{bs}}} \tag{4}$$

For the undamaged laminate, Eqs. (2-4) accurately describe the impact response of the laminate. Just before striking the laminate, the force measured by the load transducer is zero and the force increases with time, reaches a maximum and then decreases to zero. The time interval between two consecutive zero force is the impact duration. The bending-shear stiffness (k_{bs}) which is the effective spring stiffness of bending(k_b) and shear(k_s)connected in series. Because of the uncertainty of the boundary condition of the experimental set-up, the k_{bs} was experimentally measured by pressing the impact tub statically into the laminate. The stiffness (k_{bs}) for the base and interleaved laminates is 2.5 and 2.6 N/m, respectively.

By the principle of conversion of energy, the potential energy of the impact tup is converted to kinetic energy and the velocity at impact (V_0) can be expressed as:

$$V_0 = \sqrt{2gH} \tag{5}$$

Where$g$ is the acceleration due to gravity (9.81 m/s^2) and H is the impact height in meters.

The impact energy (E_0), which is the kinetic energy of the impactor of mass Mcanalso be expressed by:

$$E_0 = \frac{1}{2} M V_0^2 = E_{elastic} + E_a \tag{6}$$

where the elastic energy($E_{elastic}$)is the energy released by the target and is calculated based on the rebound acceleration, force and displacement. The dissipated energy (E_a)is the difference between E_0 and $E_{elastic}$ and is the energy used in creating damage in the laminate and the energy dissipated by the target in the form of vibration and heat, and by the impact setup in the form of inelastic behavior of the impactor and support[24, 25].

IV. TESTING

A. *Impact Testing*

The impact set-up used was a Dynatubdrop weight tower. The impactor and average laminate masses were 5.41 and 0.0641 kg, respectively. The impactor and laminate mass ratio was about 84 which is much greater than 2[24], hence the laminate mass is neglected in the analysis. The impactor mass, M, had a hemispherical tup of diameter 25.4 mm (1.0 in) and was instrumented with an accelerometer to measure the acceleration versus time response. The response is recorded by a high-speed data acquisition system. The data recorded include impact force-time, the impact force-deflection, and the energy-time responses. The tower was equipped with a pneumatic rebound brake system to prevent multiple impacts on the laminate and instrumentation to measure the velocity just before the impact.

Low velocity impact tests were conducted in accordance with the ASTM Standard D 7136. The test specimen was placed on a rigid steel frame with 76 mm x 127 mm (3 in x 5 in) rectangular cut-out test section. The specimen was centered over the cut-out by means of three guiding pins and held in place by four adjustable, rubber-tipped toggle clamps as shown in Fig. 7.The impact height, H, was set between the tip of the impactor and the top surface of the specimen (see Fig. 4a). After properly centering and clamping the specimen, the impactor was released. After impacting the specimen, the impactor re-bounces. The pneumatic rebound brake system automatically arrests the impactor and prevents multiple impacts on the specimen. Impact damage area was measured by c-scan.

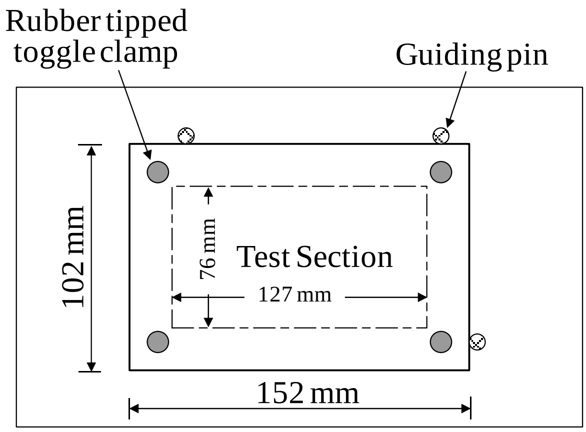

(a) Plan View

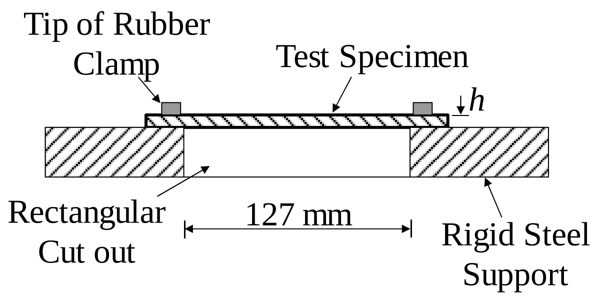

(b) Sectioned View

Figure 7 Impact test fixture and set-up

The impact acceleration Vs. time is recorded by the Dynatub data acquisition system. From that, derived quantities such as impact force, velocity, laminate central displacement and energy are calculated. Figure 8 shows the combined experimental and analytical impact responses. The analytical impact force response was obtained from Eq. (3),andit represents one-half sinusoidal wave. The duration of impact (Eq. 4) is about 4.6 ms and the maximum load (P_{max}) obtained by experimental and analytical (Eq. 3) are the same for no-damage impact.

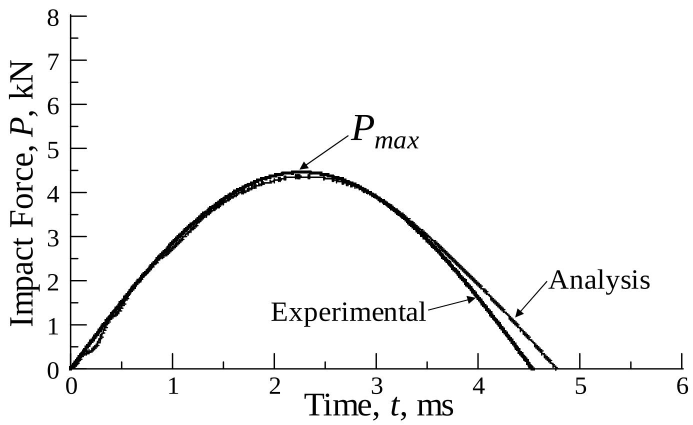

Figure 8 Typical experimental and analytical impact force-time response of an undamaged

Laminate

The impact height used in this study ranged from 57 to 254 mm. The base and the interleaved test specimens were impacted at 8 and 9 different heights, respectively. At each height, 2 or 3 specimens were impacted. The complete test matrix is shown in Table 1.

TABLE I IMPACT TEST MATRIX

H, mm	57	64	76	83	89	102	127	152	254
Base	√	√	√	√	√	√	√	√	√
Interleaved	√	√	√	√	√	√	x	√	√

B. Standard Compression Test

Baseline compression strength of the pristine quasi-isotropic base and interleaved laminates of dimensions 4.14 mm (0.163 in) x 146 mm (5.75 in) was measured according to the ASTM Standard D3410M[26] to compare the residual strength of the specimen after the impact test. The mean compression strength, F_{1C}, and standard deviation of the pristine base laminate were 650 and 21MPa, respectively, while the mean compression strength and standard deviation of the pristine interleaved laminate were 620 and 31MPa, respectively. At a confidence coefficient of 95%, there was no significant difference in the compression strength of the base and the interleaved laminates[27]. The compression strength of the pristine laminate (base or interleaved) (F_{1C}) and standard error for both the base and the interleaved laminates were calculated as 635 and 31MPa, respectively[27].

C. Compression after Impact (CAI) Test

The impact tested specimens were tested in compression according to the ASTM Standard 7137M[28]. Details of the laminate clamping and the photography of the laminate during CAI testing are shown in Fig. 9.

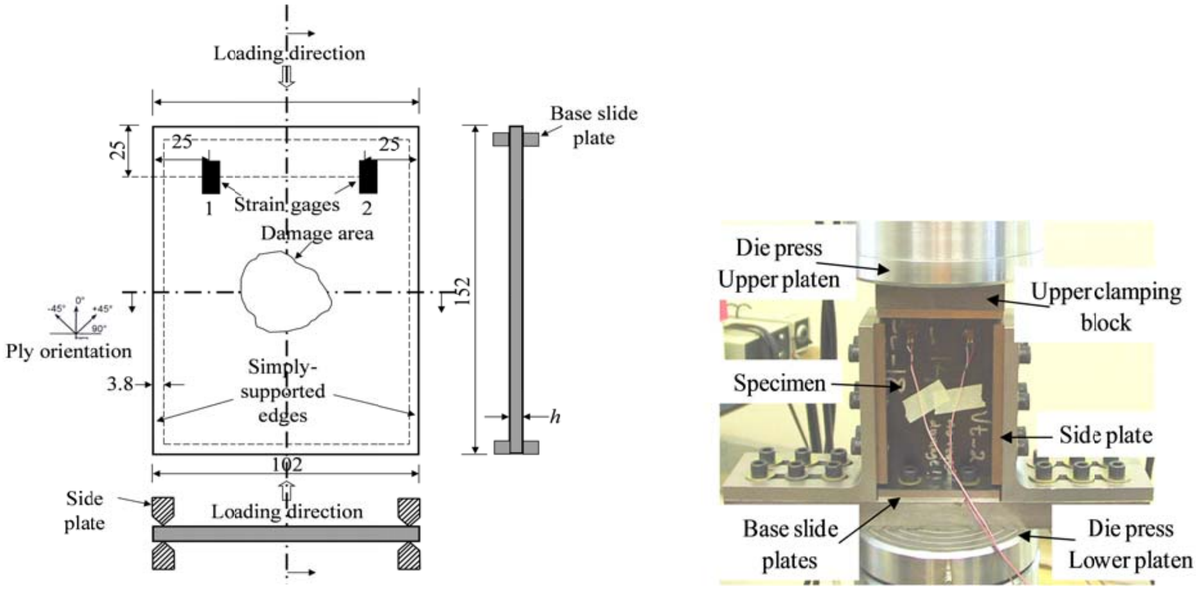

(a)Details of clamping and strain gagelocations (b)Photography of laminate during testing

Figure 9 Compression After Impact (CAI) Test

All impacted specimens were instrumented with four strain gages to measure the bending and axial strains.The locations of strain gages were towards the upper end of the specimen on both the front and back faces and they are shown in Fig. 9. Strain Gages 1 and 2 are on the front face and Gages 3 and 4 are on the back face of the specimen. The average axial strain is given by $\varepsilon_a = \frac{\varepsilon_1 + \varepsilon_2 + \varepsilon_3 + \varepsilon_4}{4}$, and the bending strain is given by $\varepsilon_b = \left| \frac{(\varepsilon_1 + \varepsilon_2) - (\varepsilon_3 + \varepsilon_4)}{4} \right|$. The percentage bending strain, at or near the maximum applied load indicates the degree of out-of-plane bending.

The CAI tests were conducted using MTS Universal Testing Machine. The impacted test specimen was mounted in the test fixture and aligned to prevent bending during testing. The specimen was supported using the side and base plates (see Fig. 9(a)), and these plates were initially secured by hand-tightening their respective screws. The upper block was gently installed on the upper edge of the test specimen. The fixture was placed gently on the lower platen of the test machine and aligned with the vertical axis of the machine. A compressive preload force of 450 N was applied to the upper block to guarantee that all the loading surfaces were in initial contact. This compressive preload force was later reduced to 150 N, the fixture screws tightened to the recommended torque of 7 Nm and then the force and strain gage readings were re-zeroed. Using the displacement control method, the specimen was loaded at the rate of 0.02 mm/s. The load, cross-head displacement and strain were recorded at every 0.2s until the specimen failed. From the load-displacement data, the maximum compression load (P_{cmax}) was extracted and used to calculate the residual compression strength (F_{CAI}).

$$F_{CAI} = \frac{P_{c\max}}{wh} \tag{7}$$

Where F_{CAI} is the residual compression strength in MPa; P_{cmax} is the maximum compressive load at failure in N, and w and h are the width and thickness of the test specimen in mm, respectively.

During the testing, loud cracking sounds could be heard as a result of matrix cracking, fiber-matrix debonding, delamination or fiber breakage. The specimen fails immediately after the maximum load was reached. It was observed that some specimen failed in compression at the impacted site while others failed in compression at the edge. Note that the specimen edge compression failure is common for low velocity impact damaged specimens.

V. RESULTS AND DISCUSSION

A. Impact Test Results

Tables 2 and 3 summarize the impact test results for the base and interleaved laminates. The tables list the specimen number, the impact height, the damage area measured by c-scan, the critical and maximum impact force (measured from the impact force Vs. time response), and the impact energies. The impact energies include initial energy (E_0), the critical energy (energy at the critical impact force, P_c), and the dissipated energy.

TABLE II IMPACT TEST RESULTS FOR BASE LAMINATES

Test Specimen ID#	Impact Height, *H*, mm	C-Scan Damage Area, D_a, mm^2	Impact Force, kN		Energy, J		
			Critical, P_c	Maximum, P_{max}	Impact, E_0	Critical, E_c	Dissipated, E_a
3_3	57	54	--	3.980	3.22	--	0.05
3_12		96	--	3.945	2.93	--	0.00
3_4	64	266	--	4.091	3.46	--	1.32
3_10		262	--	4.251	3.41	--	1.17
3_8	76	305	4.344	4.344	4.10	3.57	1.43
3_14	83	334	4.231	4.231	4.43	3.60	1.35
1_3		356	4.428	4.428	4.36	4.06	1.66
3_11	89	288	4.179	4.179	4.65	3.50	1.46
1_14		362	4.638	4.638	4.85	4.23	1.64
3_6	102	428	4.508	4.508	5.54	3.96	1.70
3_7		359	4.214	4.214	5.38	3.46	1.28
2_7		403	4.498	4.498	5.49	4.08	1.67
1_10	127	500	4.909	4.958	6.80	4.61	2.11
2_10		494	4.533	4.697	6.84	4.04	1.97
2_12		482	4.570	4.676	6.72	4.07	1.83
3_13	152	537	4.416	5.189	8.07	3.76	1.84
3_5		567	4.572	5.161	8.08	3.97	1.92
2_9		--	4.934	5.048	7.92	4.62	2.40
3_9	254	831	4.235	7.329	13.22	3.58	2.47
1_6		865	4.882	7.214	13.45	4.67	3.29
1_7		848	4.840	7.292	13.55	4.64	3.32
1_9		840	4.580	6.788	13.50	4.30	3.95
			4.5* (0.4)**			4.0* (0.7)**	

* average value

** standarderrormean

TABLE III IMPACT TEST RESULTS FOR INTERLEAVED LAMINATES

Test Specimen ID #	Impact Height, *H*, mm	C-Scan Damage Area, D_a, mm^2	Impact Force, kN		Energy, J		
			Critical, P_c	Maximum, P_{max}	Impact, E_0	Critical, E_c	Dissipated, E_a
P2_10	57	64	--	3.930	2.94	--	0.00
P1_1		100	--	3.858	2.98	--	0.00
P1_7		40	--	3.980	2.98	--	0.00
P1_14	64	70	--	4.138	3.35	--	0.00
P2_9		85	--	4.047	3.34	--	0.10
P2_14		73	--	4.074	3.32	--	0.06
P1_2	76	78	--	4.369	3.93	--	0.08
P1_6		116	--	4.477	3.87	--	0.00
P2_1		135	--	4.315	3.93	--	0.16
P2_12	83	279	4.571	4.571	4.39	4.35	1.53
P1_10		104	4.582	4.582	4.26	4.26	0.09
P1_11		103	--	4.533	4.15	--	0.00
P1_5	89	284	4.678	4.678	4.60	4.48	1.56
P1_13		289	4.705	4.705	4.61	4.43	1.52
P2_3		357	4.589	4.589	4.53	4.32	1.33
P2_4	102	405	4.717	4.717	5.46	4.58	1.70
P2_7		434	4.777	4.777	5.55	4.66	1.80
P1_4		422	4.555	4.555	5.39	4.23	1.79
P2_6	152	571	4.631	5.204	8.06	4.39	2.24
P2_8		556	4.701	5.159	7.90	4.43	2.02
P2_5		529	4.672	5.188	7.97	4.42	2.10
P1_3	254	884	4.850	7.031	13.26	4.80	5.02
P1_8		1071	4.786	7.207	13.33	4.63	3.20
P1_9		926	4.831	7.056	13.24	4.72	4.49
			4.7* (0.2)**			4.5* (0.3)**	

* average value

** standard error mean

The critical force is the force at the damage initiation[29], which is reflected in the sudden loss of stiffness[30]. From Tables 2 and 3, the average critical force and standard error mean for the base and interleaved laminate are, respectively, 4.5 kN(0.4) and 4.7 kN (0.2).It can be observed from the tables that the critical force is almost constant and independent of the impact force.

Figures 10 and 11 show the impact force Vs. time response curves for the range of impact height tested for the base and the interleaved laminates, respectively. Except for H = 57 mm, impact force-time response curves for all specimen were shifted by 2 ms for the purpose of comparing the data and for clarity. For H = 57, and 64 mm for the base laminate and, for H = 57, 64, and 76 mm for the interleaved laminate, the impact force-time response curves are smooth sinusoidal, which is a characteristic of the undamaged specimen. This response can be described by Eq. (3).

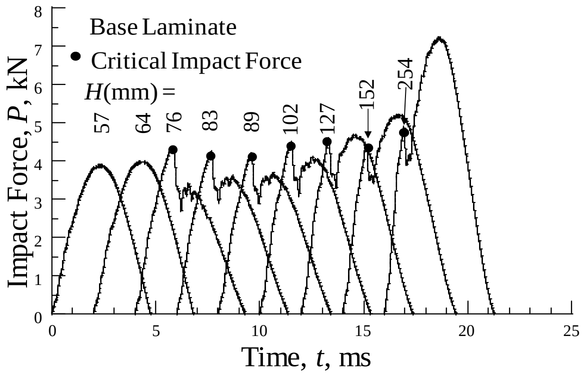

Figure 10 Impact force-time response of base laminate showing critical force

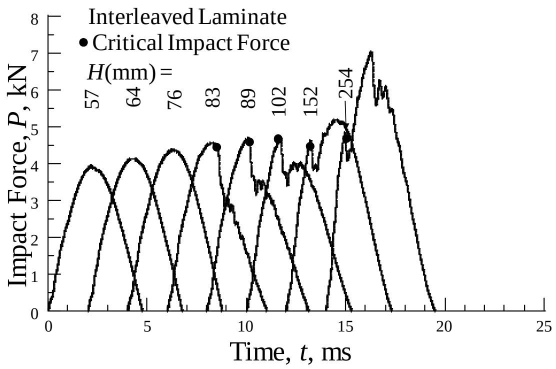

Figure 11 Impact force-time response of interleaved laminate showing critical force

However, for H = 76 mm and greater, for the base laminates, and H = 83 mm, and greater, for the interleaved laminates, the impact force-time response curves are not smooth, which is an indication of damage to various degrees. Critical force is represented by solid circle, at this force, the response curve suddenly drop. This force represents the transition from the undamaged to the damaged laminate. The associated force at these points is the critical force as previously explained.

The average critical force for the base and the interleaved laminates is plotted in Fig. 12. The standard error is specified in the plot for the base and the interleaved laminate. Polymer nanofabric interleaving increased the average critical force from 4.5 to 4.7 kN, about 4.4%.

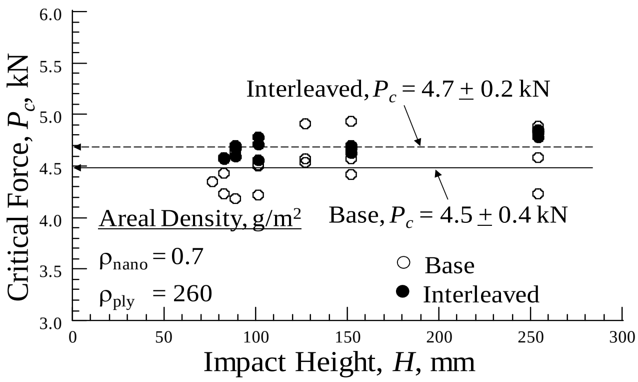

Figure 12 Critical impact force versus impact height for base and interleaved laminates

B. Damage Analysis by C-Scan

Damage resistance was ranked in terms the damage growth rate with respect to impact force and the threshold impact force. Structural Diagnostics Inc. (SDI) ultrasonic C-Scan equipment was used for assessing internal damage in the test specimens. Typical c-scan micrographs for the base and the interleaved test specimens are showed in Fig. 13.

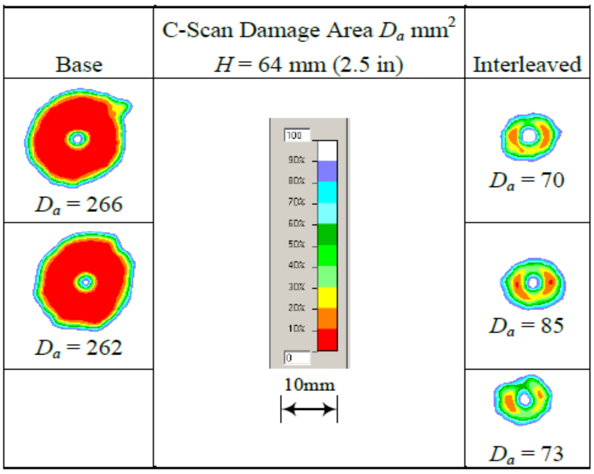

Figure 13 Typical C-Scan results at low impact height

Figure 14 shows the damage area versus impact force. The threshold impact force increased from 4.0 to 4.5 kN representing about 13% improvement (contrast with 4.5 ad 4.7 kN in Tables 2 and 3). Note that the impact threshold force is different from the critical impact force. Critical impact force corresponds to the force measured at the sudden load or compliance drop. However, the threshold force depends on the c-scan setting. In our previous preliminary study[12], the impact threshold force was increased from 1.0 to 1.6 kN, representing a 60% improvement, there the laminate was interleaved with 1.0% of the ply weight in contrast the present interleaving is only 0.27%of the ply weight.

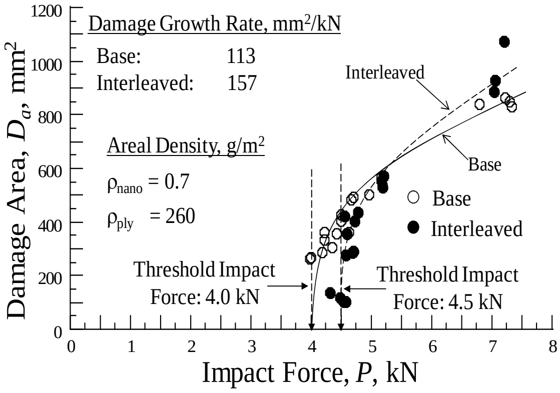

Figure 14 Damage area versus impact force for base and interleaved laminates

Figure 15 shows the damage area versus the impact energy for the base and interleaved laminates. The impact energy thresholds are 3.0 and 4.0 J, respectively, indicating an increase of 33% energy level. This modest increase may be because of the small percentage (0.27%) of Nylon 66 interleaved fibers. The threshold could be increased by increasing the percentage interleaving. The damage growth rate is almost the same for both base and interleaved composites. This trend agrees with the trend that large increase in G_{IC} compared to G_{IR} in Mode I fracture[11]. A conclusion from these results is that interleaving increases the impact damage threshold but may not increase the impact damaged growth rate.

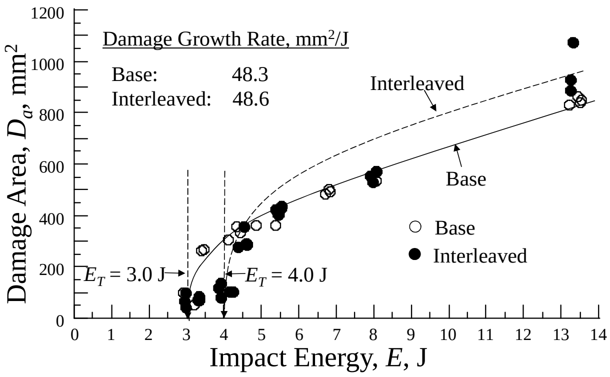

Figure 15 Damage area versus impact energy for base and interleaved laminates

C. CAI Failure Modes

Visual inspection of the compression failures sustained by the specimens indicated two major modes, edge-crushing (edge-failure) and delamination across the width of the specimen and through the impacted site in the test specimen (specimen failure). These failure types are shown in Fig. 16and Fig. 17for the base and interleaved laminates, respectively.

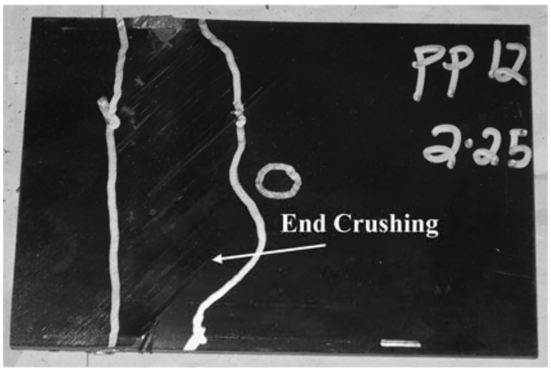

(a) Edge-crushing failure

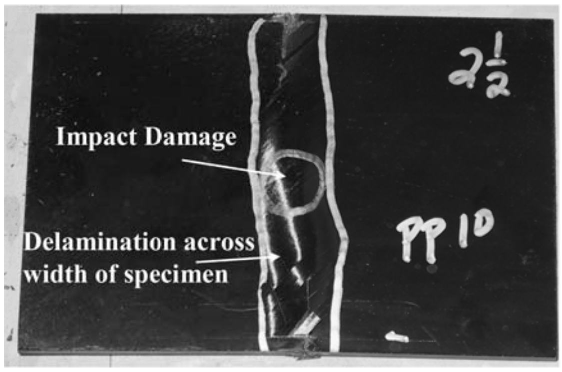

(b) Failure at impact site

Figure 16CAI failure modes for base laminate

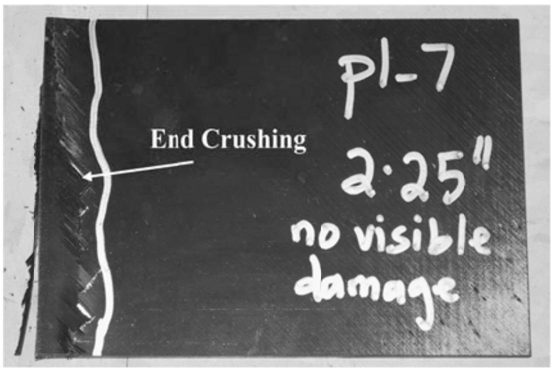

(a) Edge-crushing failure

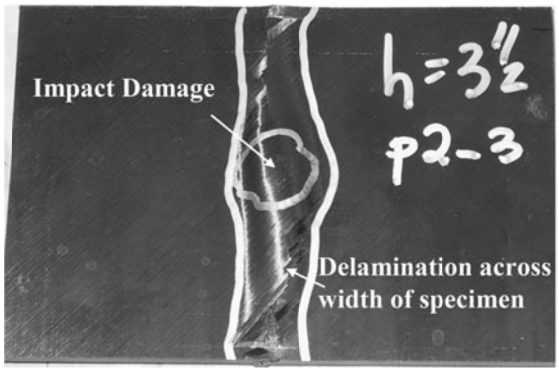

(b) Failure at impact site

Figure 17 CAI failure modes for interleaved laminate

Edge-crushing is not an acceptable failure mode, but occurred in these instances presumably because the specimens that experienced this type of failure mode were not damaged enough to cause failure at the impact site.

D. Residual Compression Strength

A typical stress Vs. cross-head displacement is shown in Fig. 18.Failureoccurred suddenly at the peak load. The residual compressive strength is calculated by dividing the failure load by the cross-sectional area as in Eq. (7). Figures 19 to 22 show the residual compressive stress for the base and interleaved laminates at various impact heights.

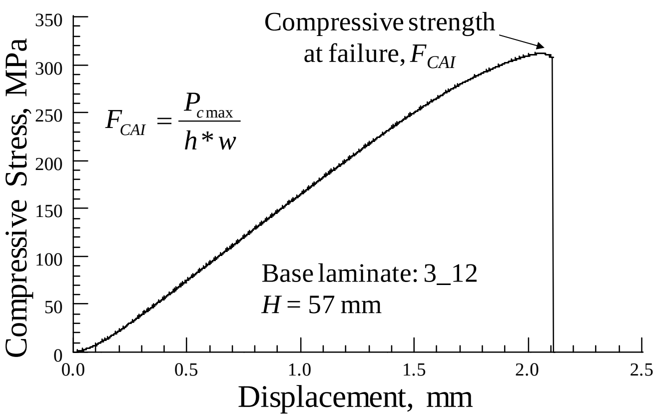

Figure 18 Typical compressive stress versus cross-head displacement for CAI test specimen

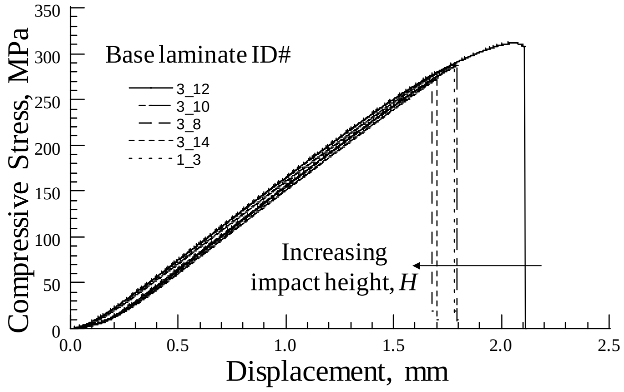

Figure 19 Base laminate compressive stress versus cross-head displacement for impact height 57 to 83 mm

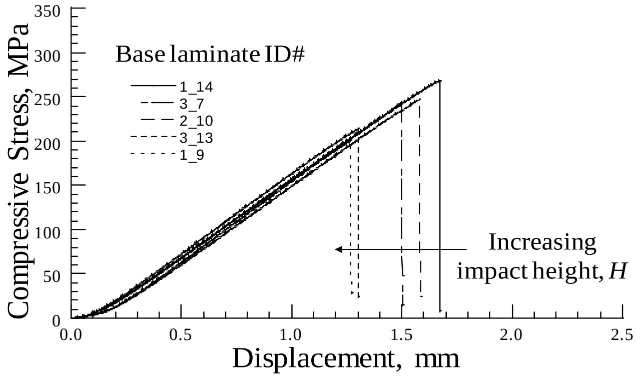

Figure 20 Base laminate compressive stress versus cross-head displacement for impact height 89 to 254 mm

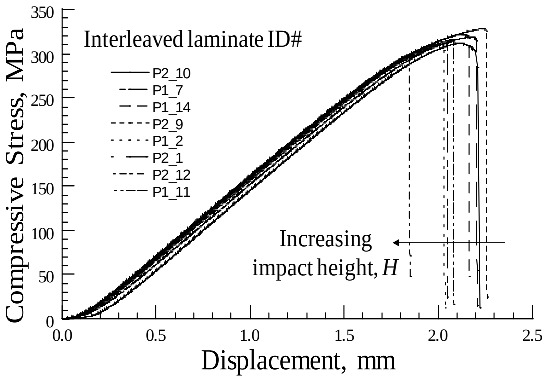

Figure 21 Interleaved laminate compressive stress versus cross-head displacement for impactheight 57 to 83 mm

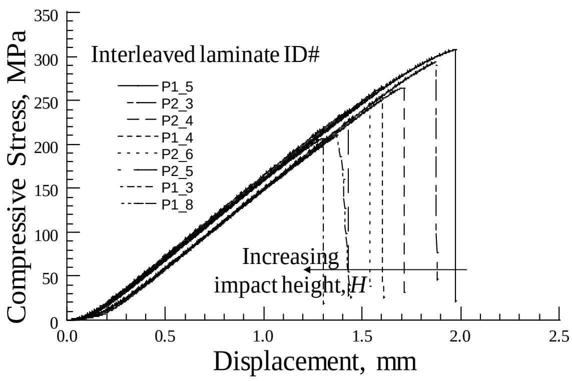

Figure 22 Interleaved laminate compressive stress versus cross-head displacement for impactheight 89 to 254 mm

Damage tolerance was assessed by the ratio of the residual compressive strength(F_{CAI}) to the average compression strength(F_{1C}) of the undamaged laminate. The average compression strength (F_{1C}) of the undamaged base and interleaved laminate was 635 MPa. The percentage bending strain in all these tests was within the $\pm$10% range allowed for in the standard. The normalized residual compression strength plotted against impact energy is shown in Fig. 23. The open symbols refer to the base laminates while the solid symbols refer to the interleaved laminates. The limit of edge compression is shown by the vertical line with a shade. The shaded region to the left of the vertical line represents the edge failure and the region on the right of the line represents the compression failure at the impacted specimen. In the compression failure region, as expected, the residual strength decreases with impact energy. The two laminates show similar trend, even though the interleaved composites have higher residual strength than the base laminate for a given impact energy. Therefore, it can be concluded that the impact damage tolerance of the interleaved composites is better but not decisively better than the base laminate.

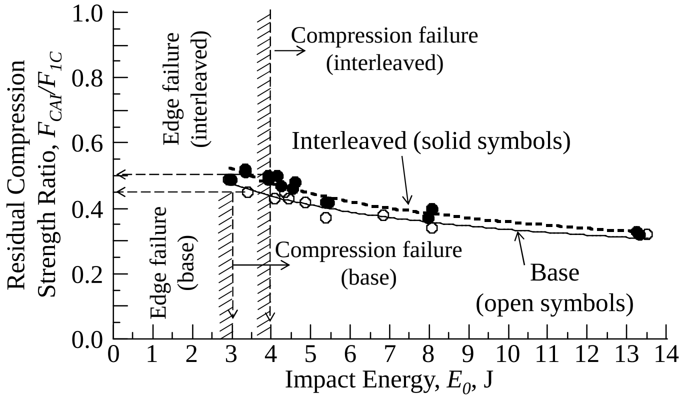

Figure 23 Residual compression strength ratioversus impact energy

The CAI test results showed that the minimum impact energy to cause the failure of the impact site was 3.0 J for the base laminate whereas it was 4.0 J for the interleaved laminate. The residual compression strength ratio increased from 0.45 to 0.50. The compression residual strength ratio decreases at increasing impact energy for both laminates.

VI. CONCLUSIONS

A 24 ply quasi-isotropic base and Nylon-66 nanofiber interleaved AS4/3501-6 composite laminates were tested in low velocity impacts to assess the impact resistance. The impacted specimens were then subjected to compression testing to assess the impact damage tolerance. The interleaving nanofabrics were prepared by electrospinning, and its areal density was 0.7 g/m^2. This areal weight translates into 0.27% of the ply weight. The impact velocity ranged from 1.03 to 2.22 m/s and the height ranged from 54 to 254 mm. The impactor mass was 5.41 kg. The following observations were made regarding the influence of interleaving on the impact damage resistance and tolerance:

1. Polymer nanofabric interleaving marginally increased the laminate thickness. This increment in thickness is unlikely to cause measurable loss of in-plane stiffness and strength of the composite as previously demonstrated by the authors.

2. Polymer nanofiber interleaving increased the threshold impact force from 4.0 to 4.5 kN, for delamination damage on-set by about 7%.

3. Polymer nanofiber interleaving increased the threshold impact energy from 3.0 to 4.0 J, an increase of 33%.

4. Residual compression strength after impact increased by about 10%, from a factor of 0.45 to 0.50, by polymer interleaving.

5. Finally, the polymer nanofiber interleaving has the potential to improve impact damage resistance and tolerance without replacing the presently utilized matrix system. However, more study is needed in optimizing the amount and dispersion of polymer the nanofibers in the composite laminate to realize the full potential and limitation.

ACKNOWLEDGMENTS

The authors wish to acknowledge grants from Army Research (W911NF0410176), NASA’s University Research Center “Center for Aviation Safety” (NNX09AV08A) and ARL-MAST (W911NF-08-2-0004). They also acknowledge the support of the ONR grant # N00014-07-1-0465.

REFERENCES

[1] O'Brien, T. K., "Towards a Damage Tolerance Philosophy for Composite Materials and Structures," Composite Materials: Tesing and

Design, American Society for Testing and Materials Special Technical Publications, No. 1059, 1990, pp. 7-13.

[2] Sela, N., and Ishai, O., "Interlaminar Fracture Toughness and Toughening of Laminated Composite Materials: A Review," Composites, Vol. 20, No. 5, 1989, pp. 423-435.

[3] Odagiri, N., Muraki, T., and. Tobukuro, K., "Toughness improved high-performance Torayca prepreg T800H/3900 Series," Proceedings of the 33rd Int. SAMPE Symp., Society for the Advancement of Material and Process Engineering. 1988. Covina, CA.

[4] Pagano, N. J., and Pipes, R. B., "The Influence of Stacking Sequence on Laminate Strength," Journal of Composite Materials, Vol. 5, No. 1, 1971, pp. 50-57.

[5] Mignery, L. A., Tan, T. M., and Sun, C. T., "The use of Stitching to Suppress Delamination in Laminated Composites", American Society for Testing and Materials Special Technical Publication, No. 876, 1985, pp. 371-385.

[6] Dow, M. B., and Dexter, H. B., "Development of Stitched, Braided and Woven Composite Structures in the ACT Program and Langley Research Center," NASA TP-97-206234, Nov. 1997.

[7] Howard, W. E., Gossard, T., Jr., and Jones, R. M., "Reinforcement of Composite Laminate Free-Edges with U-Shaped Caps", AIAA Journal, No. 86-0972, 1986.

[8] Chan, W. C., and Ochoa, O. O., "Edge Delamination Resistance by a Critical Ply Termination," Key Engineering Materials, Vol. 37, 1989, pp. 285-304.

[9] Masters, J. E., "Improved Impact and Delamination Resistance Through Interleafing," Engineering Materials, Vol. 37, 1989, pp. 317–348.

[10] Hojo, M., Matsuda, S., Tanaka, M., Ochiai, S. and Murakami, A., "Mode-I Delamination Fatigue Properties of Interlayer-toughened CF/epoxy Laminates", Composites Science and Technology, Vol. 66, No. 5, 2006, pp. 665-675

[11] Shivakumar, K., Lingaiah, S., Chen, H., Akangah, P., Swaminathan, G. and Russell, L., "Polymer Nanofabric Interleaved Composite Laminates," AIAA Jl, Vol. 47, No. 7, 2009, pp. 1723-1729.

[12] Akangah, P., Lingaiah, S., and Shivakumar, K., "Effect of Nylon-66 Nanofiber Interleaving on the Impact Damage Resistance of Epoxy/Carbon fiber Composite Laminates," Composite Structures, Vol. 92, No. 6, 2010, pp. 1432-1439.

[13] Shivakumar, K. N., Chen, H., Ali, M., “Nanofibers Interleaved Composites for Aerospace Applications,” Proceedings of the ICCCFT Conference-2011, Bangalore, India, Jan 4-7, 2011.

[14] Shin, Y. M., Hohman, M. M., Brenner, M .P., and Rutledge, G. C., "Experimental Characterization of Electrospinning: The Electrically Forced Jet and Instabilities," Polymer, Vol. 42, No. 25, 2001. pp. 09955-09967.

[15] Munir, M. M., Iskandar, F., Khairurrijal, and Okuyama, K., "A Constant-current Electrospinning System for Production of High Quality Nanofibers," Rev. Sci. Instrum., Vol. 79, 2008. pp. 093904-4.

[16] Munir, M.M., Iskandar, F., Khairurrijal, and Okuyama, K., "High Performance Electrospinning System for Fabricating Highly Uniform Polymer Nanofibers," Rev. Sci. Instrum, Vol. 80, 2009, pp. 026106-3.

[17] Yan, X. and Gevelber, M., "Investigation of Electrospun Fiber Diameter Distribution and Process Variations," Journal of Electrostatics, Vol. 68, No. 5, 2010. pp. 458-464.

[18] Samatham, R., and Kim, K. J., "Electric Current as a Control Variable in the Electrospinning Process," Polymer Engineering & Science, Vol. 46, No. 7, 2006. pp. 954-959.

[19] Theron, S. A., Zussman, E., and Yarin, A. L., "Experimental Investigation of the Governing Parameters in the Electrospinning of Polymer Solutions," Polymer, Vol. 45, No. 6, 2004. pp. 2017-2030.

[20] Fridrikh, S. V., Yu, J. H., Brenner, M. P., and Rutledge, G. C., "Controlling the Fiber Diameter during Electrospinning," Physical Review Letters, Vol. 90, No. 14, 2003. pp. 144502-4.

[21] Bhattacharjee, P. K., Schneider, T. M., Brenner, M. P., McKinley, G. H., and Rutledge, G. C., "On the Measured Current in Electrospinning," Journal of Applied Physics, Vol. 107, No. 4, 2010. pp. 044306.

[22] Fridrikh, S.V., et al., "Controlling the Fiber Diameter during Electrospinning,"Physical Review Letters, 2003. 90(14): p. 144502.

[23] Akangah, P., PhD Thesis, North Carolina Agricultural and Technical State University, 2011.

[24] Shivakumar, K. N., Elber, W., Illg, W., "Prediction of Impact Force and Duration Due to Low-Velocity Impact on Circular Composite Laminates," Journal of Applied Mechanics, Vol. 107, 1985

[25] Delfosse, D. and Poursartip, A., "Energy-based Approach to Impact Damage in CFRP Laminates," Composites Part A, Applied Science and Manufacturing, Vol. 28, No. 7, 1997, pp. 647-655.

[26] ASTM Standard D 7137/D 7137M-07, "Standard Test Method for Compressive Residual Strength Properties of Damaged Polymer Matrix Composite Plates," Annual Book of ASTM Standards, 2007, West Cronshohocken, PA.

[27] Box, G.E.P., Hunter, W.G., and Hunter, J.S.,Statistics for Experimenters: An Introduction to Design, Data Analysis and Model Building,. John Wiley & Sons,NY, (1978)

[28] ASTM standard D 3410/D 3410M-03, "Standard Test Method for Compressive Properties of Polymer Matrix Composite Materials with Unsupported Gage Section by Shear Loading," Annual Book of ASTM Standards, 2003, West Conshohocken, PA.

[29] Schoeppner, G. A., and Abrate, S., "Delamination Threshold Loads for Low Velocity Impact on Composite Laminates," Composites Part A: Applied Science and Manufacturing, Vol. 31, No. 9, 2000. pp. 903-915.

[30] Davies, G. A. O., Zhang, X., Zhou, G., Watson, S., "Numerical Modelling of Impact Damage," Composites, Vol. 25, No. 5, 1994. pp. 342-350.